Cellulose (2019) 26:6739–6754
https://doi.org/10.1007/s10570-019-02523-9

ORIGINAL RESEARCH

Paper-based electrode comprising zirconium phenylphosphonate modified cellulose fibers and porous polyaniline

Ziyang Chang · Shuangyang Li · Lijian Sun · Chunyue Ding · Xianhui An · Xueren Qian

Received: 4 January 2019 / Accepted: 22 May 2019 / Published online: 21 June 2019

Abstract Polyaniline/cellulose fibers (PANI/CFs) composite prepared by heterogeneous in situ polymerization of aniline (ANI) in the presence of cellulose fibers offered a new preparation approach for flexible paper-based electrodes. However, one problem was the undesirable and inevitable polymerization of aniline in the solution. It reduced the utilization efficiency of aniline, and therefore decreased the mass loading of PANI on CFs. Here we described a unique paper-based electrode comprising zirconium phenylphosphonate (ZrPP)-modified CFs and PANI. CFs were first in situ modified with ZrPP to enhance the binding of aniline monomer to the surface of CFs resulting in a higher utilization ratio of aniline, deposition ratio of PANI and a very promising electrode material. A conformal coating of porous PANI was formed on the ZrPP-modified CFs by a facile in situ polymerization process in water. The electrical conductivity of PANI/ZrPP/CFs composite was increased to 11.53×10^{-2} S m^{-1}. The electrochemical measurement revealed that the specific capacitance of PANI/ZrPP/CFs paper electrode was up to 321 F g^{-1} which is nearly as twice as that of PANI/CFs at a current density of 1 mA cm^{-2}. Moreover, the composite were highly environmental stability and flame retardancy compared to pure cellulose due to high mass loading of PANI induced by ZrPP. The PANI/ZrPP/CFs composite with integrate performance provided a promising paper-based electrode for energy storage.

Electronic supplementary material The online version of this article (https://doi.org/10.1007/s10570-019-02523-9) contains supplementary material, which is available to authorized users.

Z. Chang · S. Li · L. Sun · X. An · X. Qian (✉)
Key Laboratory of Bio-based Materials Science and Technology of Ministry of Education, Northeast Forestry University, Harbin 150040, People's Republic of China
e-mail: qianxueren@aliyun.com

C. Ding
Insititute of Papermaking Science and Technology, Bioengineering College, Sichuan University of Science and Engineering, Zigong 643000, People's Republic of China

Graphic abstract

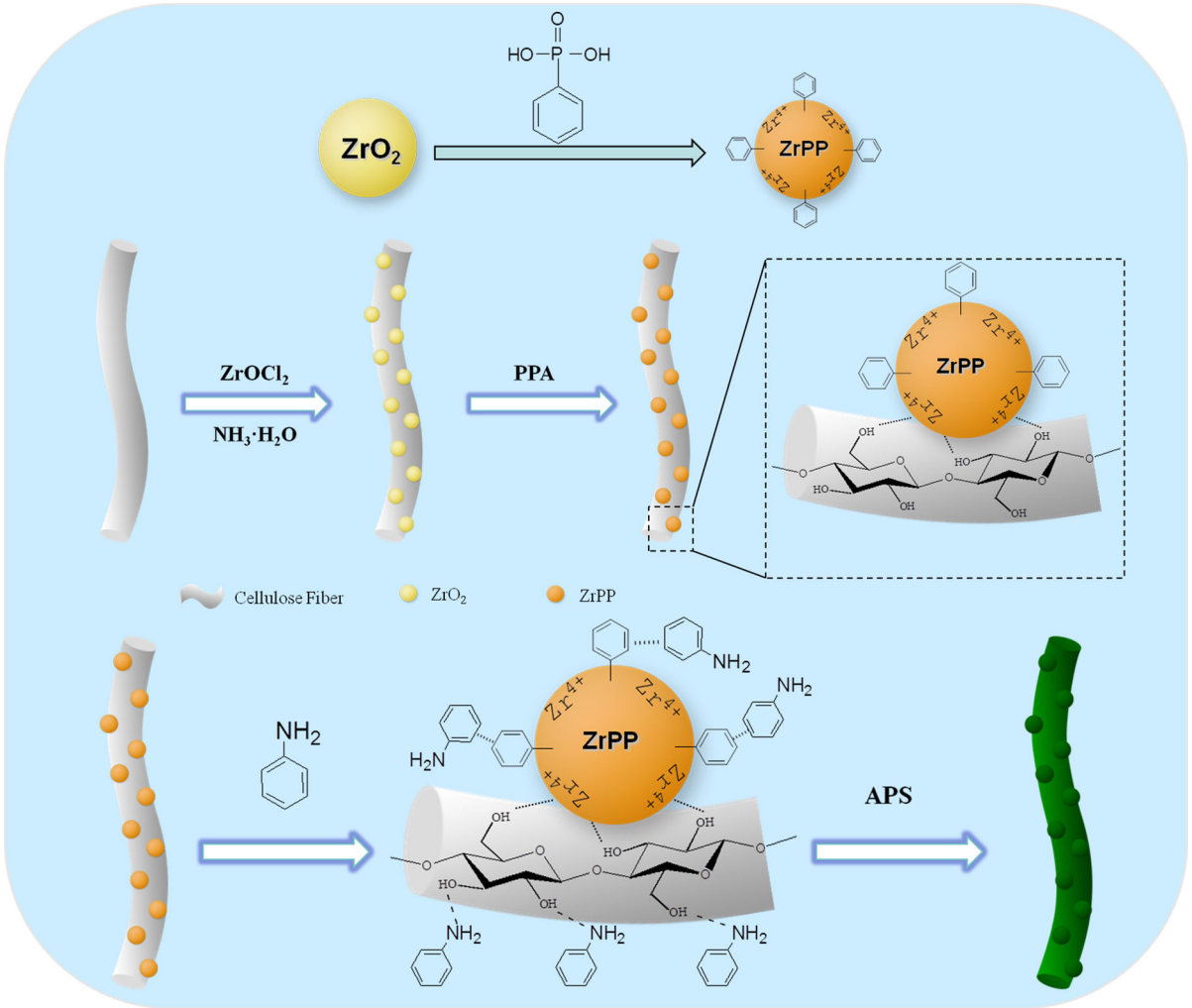

Keywords Polyaniline · Cellulose fibers · In situ polymerization · Zirconium phenylphosphonate · Paper-based electrode

Introduction

Conductive polymers are extensively studied for more than 100 years because of their unique properties and extraordinary performance (MacDiarmid et al. 1987; Tissera et al. 2018). In recent years, polyaniline (PANI), one of conductive polymers, has captured much attention due to its promising potential applications in supercapacitors (Liu et al. 2014, 2016; Park et al. 2016), sensors (Bajgar et al. 2016; Gautam et al. 2018), smart devices (de Souza Junior et al. 2014), electromagnetic interference shielding (Hu et al. 2017a), and anticorrosion coatings (Adhikari et al. 2008). As we all know, however, PANI suffers from poor processing and mechanical properties (Bober et al. 2015; Negi and Adhyapak 2002). To overcome these problems, many research efforts have been focused on depositing PANI into free-standing or porous substrates such as textile (Berendjchi et al. 2016; Maráková et al. 2017), cellulose fibers (CFs) (Goto 2010; Mao et al. 2013), and polyester (Berendjchi et al. 2016; Tang et al. 2015; Trindade et al. 2015). Among these substrates, CFs derived from wood, cotton, and agriculture by-products, as one common

polysaccharides, have the advantages of abundant reserves, renewability, reasonable price, environmental friendliness, flexibility, high concentration of active chemical moieties, high surface area and relative chemical stability (Hinterstoisser et al. 2003; Moon et al. 2011; Oksman et al. 2016; Tissera et al. 2015; Wijesena et al. 2015; Zhang et al. 2004), causing that CFs-based PANI composites (PANI/CFs) are attractive in applications of flexible electron devices (Ge et al. 2015; Hu et al. 2017b; Liu et al. 2018).

Coating of CFs with PANI could be carried out with more than one process, but recent studies were predominantly focused on in situ oxidative polymerization of aniline monomer in the presence of CFs, which is simple and efficient (Kelly et al. 2007; Liu et al. 2013; Youssef et al. 2012; Shen et al. 2016). The results of several studies have shown that pulp fibers, bacterial cellulose fibers, cotton fibers and bagasse fibers have been used to prepare PANI/CFs composites through the in situ method. Also, different solvent systems could be used to in situ prepare PANI/CFs composites (Tissera et al. 2018; Youssef et al. 2012). Moreover, in situ oxidative polymerization process has been conducted to develop numerous PANI/CFs composites for electric conduction (Sharifi et al. 2018), packing application (Youssef et al. 2012), hazardous adsorption (Avelar Dutra et al. 2017) and electrochemical energy storage (Luo et al. 2018). The past researches have reached their goals and yielded noticeable improvements of PANI/CFs composites (Mao et al. 2013, 2017). However, there are still some problems that have not been solved.

To our knowledge, PANI/CFs composites have been commonly prepared in heterogeneous system by in situ chemical polymerization process because of the extreme difficulty of cellulose fibers to dissolve in water and most common organic solvents (Mo et al. 2009; Stejskal et al. 2005). Heterogeneous in situ polymerization of aniline in the presence of CFs offered a facile approach for the preparation of flexible conductive PANI/CFs materials. However, one problem was the undesirable and inevitable polymerization of aniline in the solution, which reduced the utilization efficiency of aniline, and therefore decreased the deposition ratio of PANI. It is noteworthy that the electrical conductivity, thermostability and electrochemical properties of PANI/CFs are all deeply influenced by the content of PANI in PANI/CFs which could be effectively tuned for applications such as energy storage, electromagnetic shielding and so on (Liu et al. 2012; Mao et al. 2013). The loss of PANI not only decreases PANI deposited on CFs and utilization ratio of aniline monomer, but also reduces the electrical and electrochemical performance of PANI/CFs composites. In addition, the loss of PANI wastes chemicals and increases pressure of waste treatment, which do not accord with the tendency of ''sustainable chemistry''. Nevertheless, the problem of PANI polymerized in solution instead of on CFs was almost ignored in former reports (Mo et al. 2009; Sharifi et al. 2018; Youssef et al. 2012), and seldom researches were focused on the utilization ratio of aniline in the preparation of PANI/CFs composites.

In this study, we described a unique conductive CFs composite with ZrPP and PANI. CFs were first in situ modified with ZrPP to enhance the binding of aniline monomer to the surface of CFs resulting in a higher utilization ratio of aniline, deposition ratio of PANI and a very promising electrode material for supercapacitor. A conformal coating of porous PANI was formed on the ZrPP-modified CFs by in situ polymerization of aniline monomer. Compared with PANI/CFs, the electrical conductivity of PANI/ZrPP/CFs was increased by more than ten times. Moreover, the ZrPP on CFs was critical to improve the environmental stability and flame retardency of the PANI/ZrPP/CFs composite. The electrochemical measurement revealed specific capacitance of PANI/ZrPP/CFs paper sample was nearly as twice as that of PANI/CFs at a current density of 5 mA cm^{-2}. Furthermore, the composite could be used as other fields such as flexible energy storage, antistatic packing and electromagnetic shielding.

Experimental section

Materials

Aniline of chemical grade was freshly distilled under reduced pressure (− 0.1 MPa), and was then stored in a refrigerator at 4 °C prior to use. Fully bleached softwood kraft pulp (i.e., CFs) was obtained from Mudanjiang Hengfeng Paper Co. Ltd., PR China. The pulp board was soaked overnight in distilled water at room temperature and then beaten to a beating degree of 39 °SR at a consistency of 1.6% in Valley beater (Xianyang Test Equipment Co., Ltd). Finally, the wet

pulp was dewatered and sealed in a plastic bag for further use. All the other chemicals, including ammonium persulfate (APS, $(NH_4)_2S_2O_8$), sulfosalicylic acid (SSA), ammonium hydroxide solution (25–28% NH_3), zirconyl chloride octahydrate ($ZrOCl_2{\cdot}8H_2O$) and phenylphosphonic acid (PPA, $C_6H_5PO(OH)_2$), were of analytical grade, and were used as received. All the solutions were prepared from distilled water.

Preparation of ZrPP/CFs

Two grams of CFs (oven-dry basis) were uniformly dispersed with 150 mL $ZrOCl_2$ aqueous solution with certain concentration in a 250 mL three-neck flask, and then 50 mL 1.5% ammonium hydroxide solution was dropwise added into the reaction system slowly. After stirring for 60 min, the CFs with white precipitate were filtrated and sufficiently washed. The composite was uniformly redispersed in 200 mL 0.05 M PPA and stirred for 60 min, then washed until the filtrate was colorless and neutral. The composite was named as ZrPP/CFs.

Preparation of PANI/ZrPP/CFs

PANI/ZrPP/CFs composites were prepared according to the previous report with minimal modifications (Mao et al. 2013). The detailed procedure is presented as follows: ZrPP/CFs were placed in a three-neck flask in an ice bath and then 150 mL 0.4 M SSA solution was poured into the flask to keep fibers evenly dispersed. Subsequently, certain amounts of aniline monomer were added to the above dispersion. After stirring for 20 min, 50 mL ammonium persulfate (APS) solution (dissolved in 0.4 M SSA solution) was dropwise added into the reaction system slowly to start the oxidation polymerization reaction. The molar ratio of aniline monomer to ammonium persulfate was 1:1. The reaction was conducted with continuous stirring for 120 min. Finally, the suspension was filtered through a nylon filter bag (100 meshs) and washed with tap water several times until the filtrate was colorless. And then a handsheet with a grammage of over 60 g m^{-2} was made on a ZCX-200 handsheet former. The handsheet was pressed at 0.8 MPa for 5 min and dried at 105 °C for 10 min (5 min each side). The handsheet named as PANI/ZrPP/CFs was conditioned at 23 °C and 50% relative humidity for 24 h before testing. The control sample of PANI/CFs was prepared at the same conditions of PANI/ZrPP/CFs in the absence of ZrPP.

Characterization

The surface morphologies were characterized by means of scanning electron microscopy (SEM) (JSM-7500F, JEOL, Japan) analysis at various magnifications. The samples were attached on the microscope stage with double-sided conductive tape and were further sputtered with gold to avoid charging and get good electrical contact. The elemental compositions of the samples were determined with an energy dispersive spectrometer (EDS, USA) attached to the SEM. ATR-FTIR spectra were collected over a range of 550–4000 cm^{-1} on a Thermo Fisher Scientific Nicolet 6700 spectrometer with a resolution of 4 cm^{-1} and scanning frequency of 32 times.

Measurement of electrical conductivity (k)

The bulk resistivity of the paper samples was measured by an RTS-8 four-point probe resistivity apparatus (4Probes Tech. Co., China) and expressed as ρ (kΩ cm). Since the bulk resistivity is related with the dimension of paper samples, the thickness (T) and basis weight (W) were measured beforehand.

The conductivity expressed as k was the inverse of the bulk resistivity (ρ), which was expressed in SI unit of Siemens per meter (S m^{-1}), and was calculated as follows:

$$k = \frac{1}{10\rho} \tag{1}$$

Calculation of utilization ratio (UR) of aniline

The utilization ratio of aniline was expressed as UR (%), which was determined according to the following equation:

$$UR = (m_2 - m_1)/m_0 \times 100\% \tag{2}$$

where m_0 is the mass of doped PANI prepared without CFs, g; m_1 and m_2 are the masses of the paper samples made from the CFs or modified CFs before and after PANI deposition, respectively, g.

Calculation of PANI deposition

The amount of PANI deposited on CFs was expressed as deposition ratio (D, %), which was determined according to the following equation:

$$D = [(W - W_0)/W_0] \times 100\% \quad (3)$$

where W_0 and W are the basis weight of the handsheets made from the CFs or modified CFs before and after PANI deposition, respectively, g m^{-2}.

Measurement of oxygen index

Paper flame retardancy was determined in terms of the oxygen index, which was measured on a JF-3 oxygen index meter made in China. The paper sample was cut into strips (120 mm × 15 mm), and then the strip was placed in the combustor, where a mixture of oxygen and nitrogen flows upwards. The volume content of oxygen was adjusted to keep the lowest oxygen concentration which just supported sustained burning. The oxygen index was expressed in volume percentage. Generally, an oxygen index of more than 25% is considered to be satisfactory for flame retardancy of paper products (Mao et al. 2013; Wu et al. 2013).

Electrochemical measurements

All electrochemical tests of the paper electrodes were carried out in 1.0 M H_2SO_4 at room temperature using CHI660E electrochemical workstation (Chenhua Instrument, Shanghai, China). The paper sheets were cut into small square slices with a typical area about 10 mm × 10 mm and then clamped in a polytetrafluoroethylene chuck with a platinum plate as working electrodes. A platinum plate and a Ag/AgCl were used as counter and reference electrodes, respectively. The cyclic voltammetry (CV) measurements were carried out at various scan rates in the potential range from − 0.1 to 0.9 V. Galvanostatic charge–discharge (GCD) property was conducted over the potential range from − 0.1 to 0.9 V at various current densities.

The gram-specific capacitances of paper electrodes were calculated from GCD curves according to the equation:

$$C_m = \frac{I \times t}{(\Delta V - IR_{drop}) \times m} \quad (4)$$

where C_m is gram-specific capacitance calculated from charge–discharge curves, I is charge or discharge current (A), t is the time for full discharge (s), and ΔV is the potential window, IR_{drop} is the IR voltage drop, and m is the mass of electroactive material in the working electrode.

Results and discussion

Preparation process of composites

The incorporation of ZrPP into CFs can be described by the following two reactions:

Step 1: $CFs + ZrOCl_2 + NH_3{\cdot}H_2O \rightarrow ZrO_2/CFs + NH_4Cl$

Step 2: $ZrO_2/CFs + C_6H_5PO(OH)_2 \rightarrow ZrPP/CFs + H_2O$

The ZrO_2 particles were deposited on the CFs surface through the electrostatic interactions between Zr ions and hydroxyl groups of CFs. After adding phenylphosphonate acid (PPA), ZrO_2 was changed to ZrPP because of its high adsorption capacity for phosphoric acid (Borgo and Gushikem 2002). The deposition of ZrPP on the CFs formed a Zr ions and phenyl-tagged CFs surface (Scheme 1). The mass percentage of ZrPP in ZrPP/CFs was about 6.60% by comparing the weights of handsheets which were prepared by CFs before and after ZrPP modification.

To impart conductivity to ZrPP/CFs composites, PANI was in situ synthesized and deposited on CFs which were served as flexible substrates for PANI deposition. First, aniline monomer was added to the suspension of ZrPP/CFs and adsorbed on ZrPP/CFs. Amine groups of aniline monomer formed hydrogen bonds with the hydroxyl groups of CFs (Hu et al. 2011), and phenylic rings on the aniline monomer formed π–π interactions with the phenylic rings of ZrPP. After oxidant solution of APS was added, PANI particles were synthesized and deposited on both CFs and ZrPP.

The issue of utilization ratio of aniline which has not been investigated in former researches was studied and the results was presented in Fig. 1a. The utilization ratio of aniline monomer was increased with the increase of $ZrOCl_2$ dosage due to the ZrPP modification. Figure 1a shows the relationship between $ZrOCl_2$

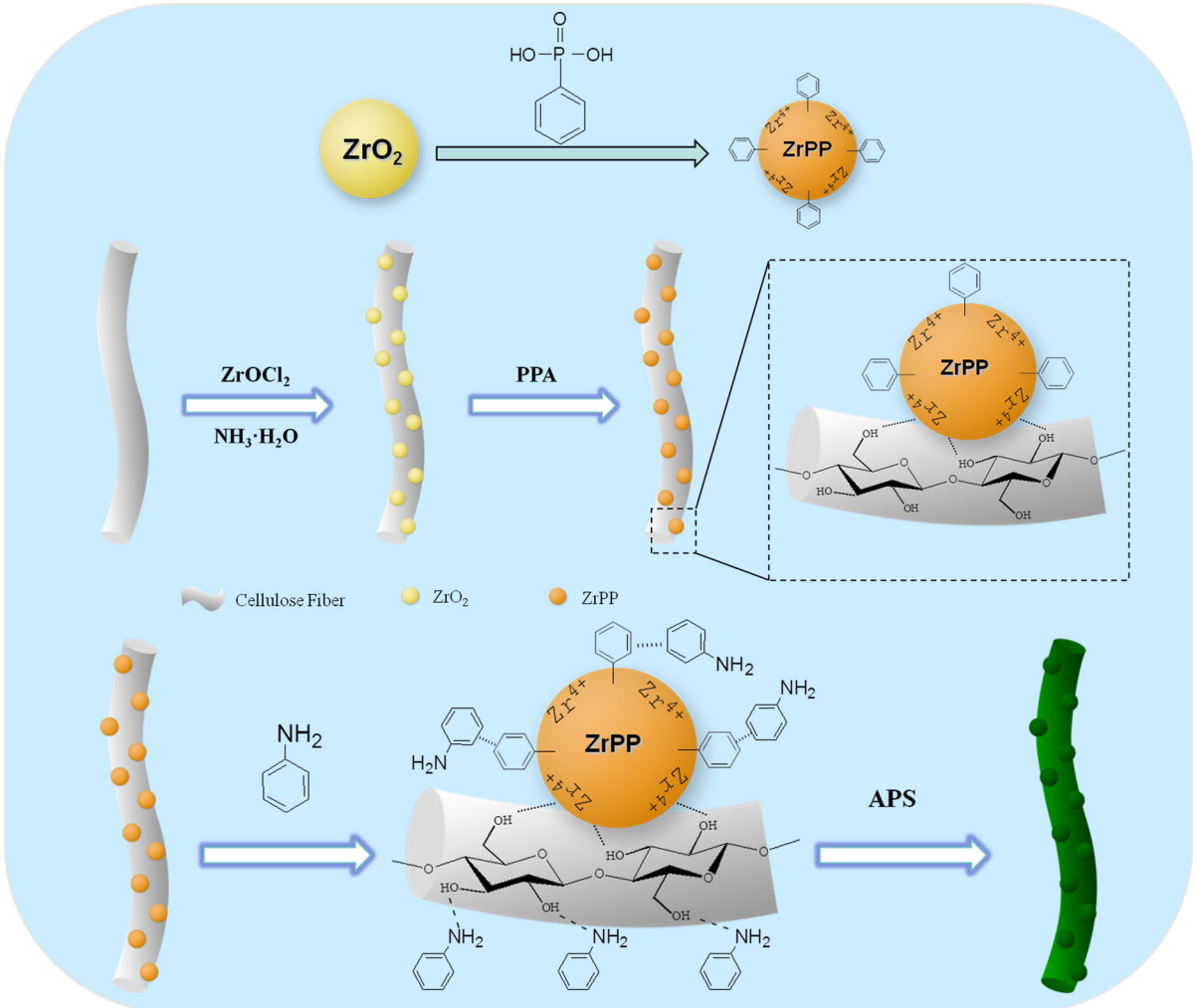

Scheme 1 Preparation of ZrPP/CFs and PANI/ZrPP/CFs

dosage and utilization ratio of aniline. The utilization ratio of aniline was about 19.79% in the absence of ZrPP which was relatively low compared to ZrPP used. The utilization ratio of aniline was increased to 76.21% when 0.002 mol $ZrOCl_2$ was added. However, when $ZrOCl_2$ dosage was increased to 0.008 mol, the utilization ratio of aniline was decreased to about 71.74% which was still well above that of the composite without ZrPP. It may be because the capacity of CFs to absorb aniline was improved by ZrPP as $ZrOCl_2$ dosage was increased. However, the content of ZrPP was too much to attach tightly to CFs when $ZrOCl_2$ dosage was further increased. The deposition ratio of PANI was determined by comparing the weights of ZrPP/CFs and PANI/ZrPP/CFs paper samples. Figure 1b shows the relationship between $ZrOCl_2$ dosage and deposition ratio of PANI as well as electric conductivity of paper samples. About 11.14% deposition ratio of PANI was achieved for the CFs without ZrPP, which is similar to the previous research (Sharifi et al. 2018). More than 45% deposition ratio of PANI was achieved for ZrPP/CFs at 0.002 mol $ZrOCl_2$ dosage, which is about four times higher than that of the CFs without ZrPP.

As we all know, CFs are intrinsically non-conducting; however they become conductive after the PANI coating. The conductivity of the PANI/CFs prepared without ZrPP was about 0.05×10^{-2} S m^{-1} (Fig. 1b). The conductivity of PANI/ZrPP/CFs was reached to 3.4×10^{-2} S m^{-1} when $ZrOCl_2$ dosage

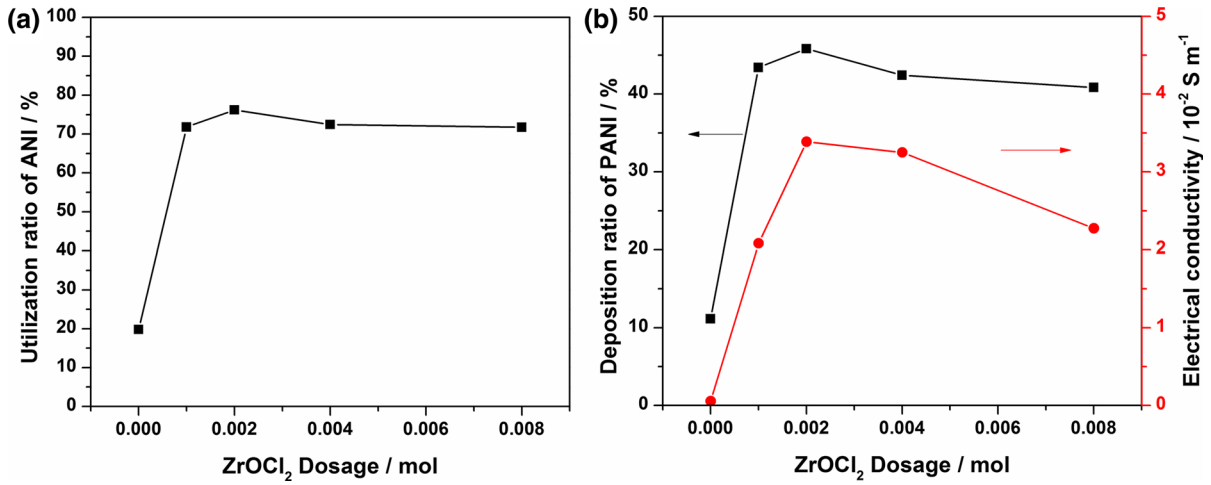

Fig. 1 Change of the utilization ratio of aniline with $ZrOCl_2$ dosage (**a**), Change of the deposition ratio of PANI and electrical conductivity of PANI/ZrPP/CFs with $ZrOCl_2$ dosage (**b**)

was increased to 0.002 mol. And it was less reduced when $ZrOCl_2$ dosage was further increased to 0.006 and 0.008 mol. It may be due to the mass variation of PANI which was affected by the content of ZrPP attached to CFs.

Morphology of composites

Compared to the surface of CFs modified with ZrPP, the surface of original CFs was quite smooth and clean (Fig. S1). After ZrPP deposition, the toughness of CFs surface increased significantly (Fig. 2). The toughness of CFs surface played an important role to promote the polymerization of aniline on CFs. In addition, PANI was successfully coated on the surface and interspaces of ZrPP/CFs. The irregular PANI particles were agglomerated into clusters with different sizes on original CFs (Fig. 2c, d). The morphology of PANI/ZrPP/CFs (Fig. 2e, f) was different from PANI/CFs because of the presence of ZrPP. The sizes of PANI particles were smaller and more uniform. It also can be seen that the surface of ZrPP/CFs was fully coated with PANI and the particles were tightly attached to ZrPP/CFs. Thus, we could infer that ZrPP promoted the deposition of PANI on CFs. The 3-dimensional porous structure of PANI layer which was obviously observed was expected to increase the specific area of paper-based electrodes and speed up the electron transfer, possibly giving rise to improved electrochemical activity and thermostability of the composite. In addition, the presence of Zr and P elements in PANI/ZrPP/CFs composite was confirmed by the energy dispersive X-ray spectrum (EDS) data in Fig. 2g, which indicated the existence of ZrPP in the composite.

FTIR analysis of composites

The FTIR spectra of CFs, ZrPP/CFs, PANI/CFs and PANI/ZrPP/CFs are shown in Fig. 3. The spectrum of CFs shows the representative features of cellulose (Fig. 3a). There was a broad band attributed to O–H stretching vibration around 3300 cm^{-1} as well as a peak assigned to C–H stretching vibration around 2880 cm^{-1} (Mao et al. 2015). The strong absorption bands around 1160, 1106, 1050 and 1020 cm^{-1} come from the overlapping bands were assigned to the C–O, C–C and C–O–C stretching vibrations. In the spectrum of ZrPP/CFs (Fig. 3b), the characteristic peaks of CFs around 3300, 2880 and 1160 cm^{-1} were clearly observed. And changes in the spectrum could also be observed around 693 and 748 cm^{-1} which were served as signature bands for the phenylphosphonate group (Stein et al. 1996). After PANI deposition (Fig. 3c, d), some new peaks appeared in comparison with the former spectrum. The characteristic peaks at 1487 and 1579 cm^{-1} were assigned to the C=C stretching modes of the benzenoid ring and the quinoid ring, respectively, which indicated the oxidation state of PANI. The peak at 1300 cm^{-1} was corresponded to the C–N stretching vibration of the secondary aromatic amine. These results were in

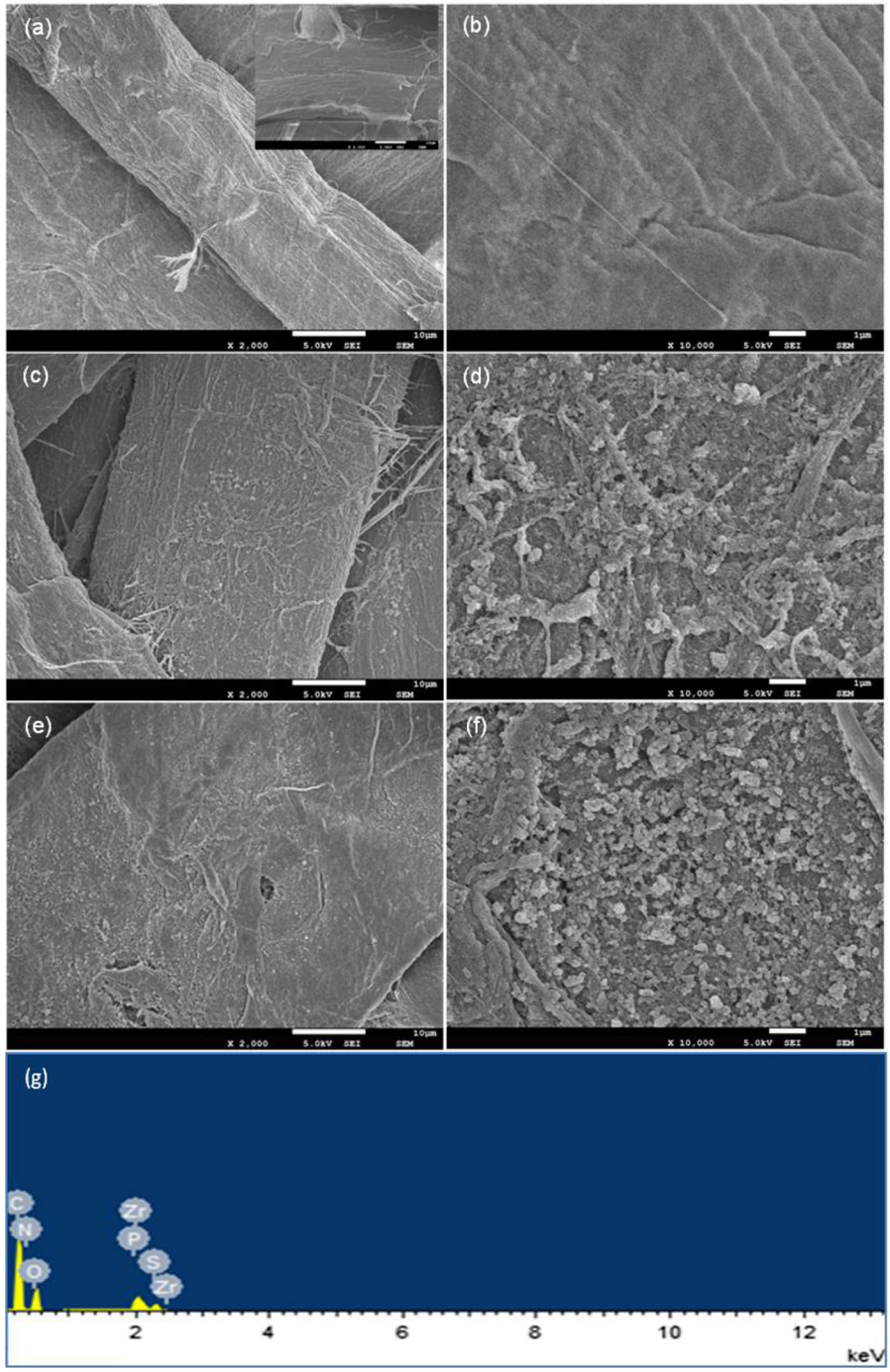

Fig. 2 Original CFs (inserted in a), ZrPP/CFs (**a**, **b**), PANI/CFs (**c**, **d**), PANI/ZrPP/CFs (**e**, **f**) and EDS spectrum of PANI/ZrPP/CFs (**g**)

agreement with those in previous reports for PANI (Mao et al. 2017). Compared with the FTIR spectra of PANI/CFs and ZrPP/CFs, the vibration bands of PANI/ZrPP/CFs assigned to the characteristic bands for PANI and ZrPP were found. However, there were several differences among the spectra. As is commonly observed, the peaks of PANI in PANI/ZrPP/CFs were stronger than those in PANI/CFs, which revealed that the PANI in PANI/ZrPP/CFs was richer than that in PANI/CFs. This also suggested that ZrPP

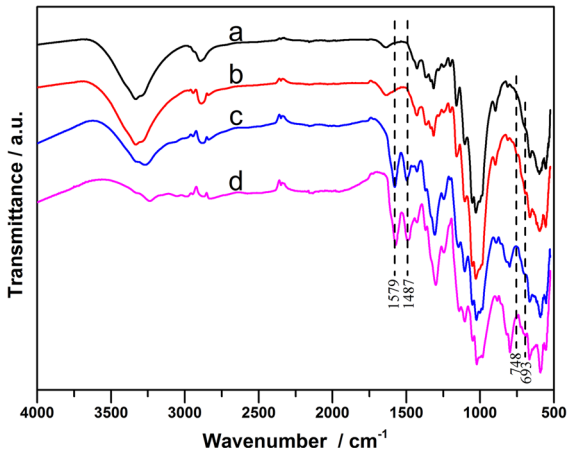

Fig. 3 FTIR spectra of CFs (**a**), ZrPP/CFs (**b**), PANI/CFs (**c**), and PANI/ZrPP/CFs (**d**)

might interact strongly with the conjugated structure of PANI, especially through the quinod ring (Liu et al. 2011).

Effect of polymerization time

PANI/CF and PANI/ZrPP/CFs composites were prepared at different polymerization times (90, 120, 150, 180 and 210 min), and the influence of polymerization time on the utilization ratio of aniline and the conductivity of composites are shown in Fig. 4. The utilization ratio of aniline in the preparation of PANI/CFs and PANI/ZrPP/CFs increased at first and then remained unchanged with the increase of polymerization time (Fig. 4a). It is noteworthy that the utilization ratio of aniline for PANI/CFs was reached to about 40.69% at 150 min, but that for PANI/ZrPP/CFs was increased to 78.85% at 120 min. As shown in Fig. 4b, the polymerization time dependence of PANI deposition ratio showed a similar change tendency with that of aniline utilization ratio. The deposition ratio of PANI on PANI/ZrPP/CFs was reached to the maximum value of 44.72% at 120 min, and that of PANI on PANI/CFs was reached to maximum value of 24.60% at 150 min. It means the mass loading of PANI on ZrPP/CFs was significantly increased because of the affinity of ZrPP to PANI. As shown in Fig. 4c, the conductivity of PANI/ZrPP/CFs increased at first and then decreased with the increase of polymerization time. The conductivity of PANI/ZrPP/CFs reached to the maximum value of 11.53×10^{-2} S m^{-1} at 180 min, which was much higher than that of PANI/CFs (0.82×10^{-2} S m^{-1}). It was possibly because the phenylic rings of ZrPP and PANI produced a weak electric field (Liu et al. 2011). ZrPP increased the overlapping degree of the π electron cloud in the PANI molecules conjugate plane, and the phenylic ring, which stretched out of the ZrPP/CFs surface, increased the density of the π electron; this was equal to the increase in the number of conductive carriers, which accelerated π–π electron transition in the PANI chains and reduced the electrical conductance activation energy in a certain range. Simultaneously, there were π–π interactions between the ZrPP and the quinoid ring of PANI molecular chain under such condition, which could improve the deposition of PANI on ZrPP/CFs. Thus, more electrical pathways were formed by the large amounts of PANI network. This efficiently promoted the transmission of electrons on the PANI chains, and resulted in an increase in the electrical conductivity of PANI/ZrPP/CFs.

Effect of varies modifications of CFs

In order to further demonstrate the interaction between ZrPP and PANI as well as its effect on aniline utilization ratio, PANI deposition ratio and conductivity, PANI/ZrO_2/CFs and PANI/PPA/CFs were prepared to compare with PANI/ZrPP/CFs and PANI/CFs, respectively. The results shown in the Fig. 4d–f are all indicated that ZrPP plays a key role to the properties of PANI/CFs which might attribute to the phenylic ring of PPA. On the one hand, π–π interactions between PPA (ZrPP) and PANI molecular chain could enhance the adhesion ability of ZrPP/CFs to PANI. On the other hand, the phenylic ring of ZrPP (PPA) could enhance the density of electron cloud in PANI molecules conjugate plane and accelerate the electron transition which caused the higher conductivity. However, it was found that the property of PANI/ZrO_2/CFs was not as well as the others, which might be due to the loosely state of ZrO_2 flocculation. The flocculated ZrO_2 was more hydrophilic and loose than ZrPP, so it was easy to be divorced from the CFs. Thus, a part of PANI/ZrO_2 particles showed the tendency of dispersing into solution other than attaching to CFs during stirring, and lost during filtration and washing process. The presence of ZrO_2 decreased the PANI deposited on CFs and conductivity of PANI/CFs. The other part of ZrO_2 was deposited on CFs through the electrostatic interactions. It is

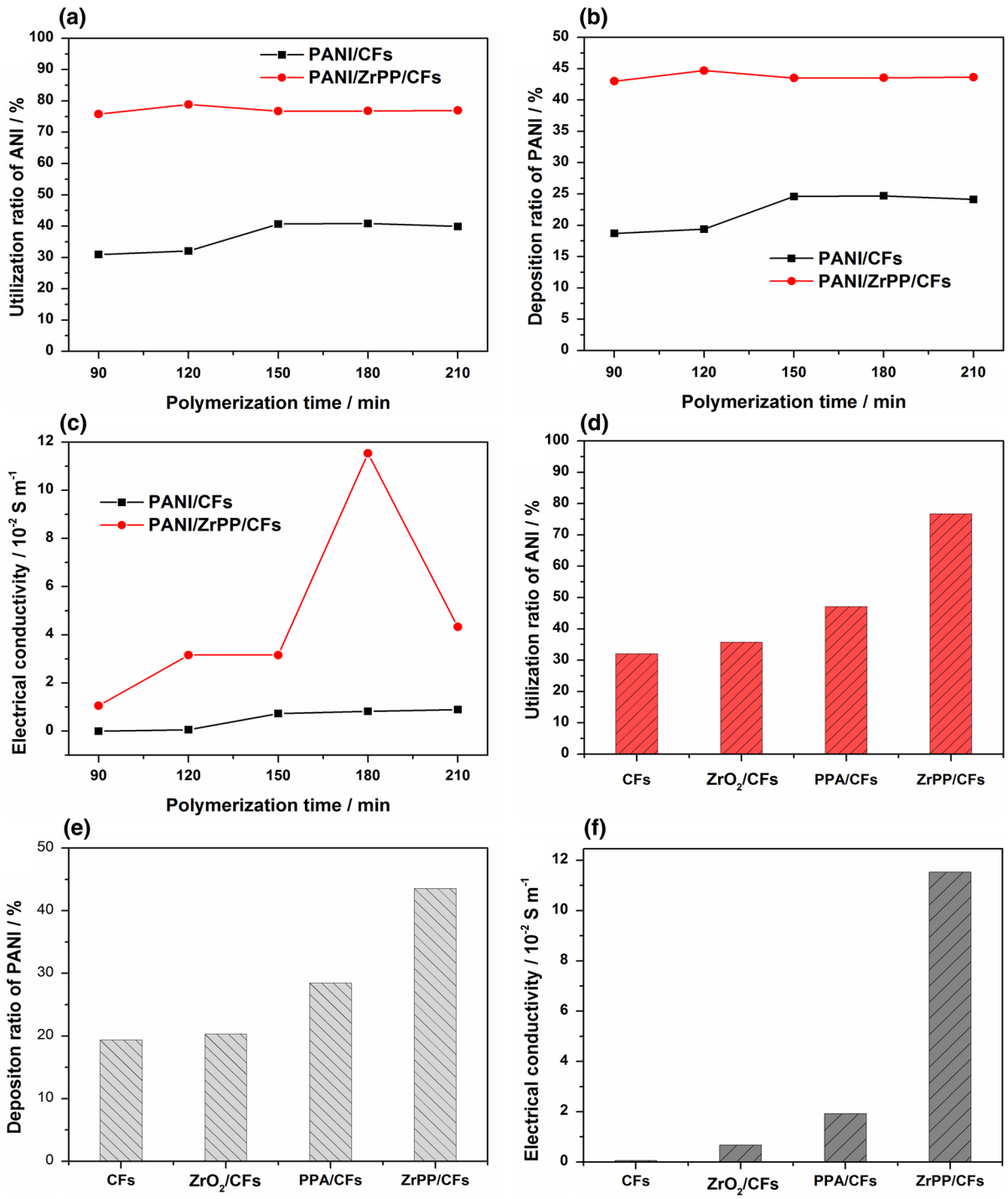

Fig. 4 Changes of utilization ratio of aniline (**a**), deposition ratio of PANI (**b**) and conductivity of composites (**c**) with polymerization time; Utilization ratio of aniline (**d**), deposition ratio of PANI (**e**) and electrical conductivity of composite (**f**) with various substrates

noteworthy that the ZrO_2 was binded with PPA and transformed to ZrPP on the surface of CFs after adding PPA, which brought abundant active groups to CFs. In addition, the roughness of the CFs surface was increased because of the deposition of ZrPP. Both the active groups and the roughness made contribution

to improving the properties of PANI/ZrPP/CFs, which was consistent with the previous analysis.

Effect of aniline dosage

Table 1 shows the properties of PANI/CFs and PANI/ZrPP/CFs with different aniline dosages. Only 11.65% deposition ratio of PANI was achieved for the PANI/CFs prepared at 0.5 mL aniline dosage. However, the deposition ratio of PANI was increased to about 23.88% for the PANI/ZrPP/CFs prepared at the same aniline dosage. The similar pattern could be observed from Table 1 when 1 mL aniline was used. The utilization ratio of aniline in PANI/ZrPP/CFs preparation was more than two times higher compared to that of PANI/CFs when 1 mL aniline was used. The results indicated that ZrPP played an important role in the increment of deposition ratio of PANI as well as the utilization ratio of aniline.

The PANI/CFs composite prepared at 0.5 mL aniline dosage was insulator, which indicated that the PANI in the composite was too less to form conductivity network. However, it became conductive after ZrPP incorporation. Furthermore, the PANI/ZrPP/CFs composite prepared at 1 mL aniline dosage became highly conductive, and its conductivity was 20 times of the PANI/ZrPP/CFs composite prepared at 0.5 mL aniline. The excellent conductivity of PANI/ZrPP/CFs could be related to the compact PANI network.

Environmental stability of composites

PANI/ZrPP/CFs and PANI/CFs samples were stored in natural environment and the changes of the electrical conductivity values with storage time were measured to investigate the environmental stability. As shown in Fig. 5a, the conductivity of PANI/ZrPP/CFs and PANI/CFs were both decreased gradually during the first 14 days, but remained basically unchanged thereafter. PANI/CFs only retained about 53% of the original conductivity. The decay of both the conductivity of the composites in atmosphere were due to the dedoping of the polyaniline deposited on cellulose fibers. However, PANI/ZrPP/CFs remained more than 80% of the original conductivity although its conductivity was decreased from 11.53×10^{-2} to 9.65×10^{-2} S m^{-1}. In comparison with the conductive paper samples without ZrPP, the paper samples with ZrPP has better environmental stability, which may attributed to the organic acid absorbed in ZrPP particles was released in a gradual way and acted as doping agent in the chains of PANI.

Flame retardancy of composites

In order to evaluate the effect of ZrPP on the flame retardancy property of PANI/CFs, the oxygen index of PANI/ZrPP/CFs composite was compared with that of PANI/CFs and CFs. As shown in Fig. 5b, the oxygen index values of papers made from CFs and PANI/CFs were 19.8% and 20.8%, respectively. However, the oxygen index value was increased dramatically, reached to 26.2% after ZrPP incorporation, which was higher than 25% (the satisfactory value for flame retardancy of paper products). As shown in Fig. 5b, there was an obvious increase in the utilization ratio of aniline after ZrPP incorporation, the deposition ratio of PANI in PANI/ZrPP/CFs was increased by more than three times (72.62%) compared to that of PANI/CFs without ZrPP (19.79%).

The above results indicated that the oxygen index values of composites as well as utilization ratio of aniline had a close relationship with the incorporation of ZrPP, which was consistent with the previous analysis. The good flame retardancy property may due to the higher content of PANI in PANI/ZrPP/CFs than PANI/CFs. It suggested that PANI can be considered as a flame retardant agent. This finding is in concordance with the previous report (Mao et al. 2013). In

Table 1 Effect of aniline dosage on the properties of PANI/CFs and PANI/ZrPP/CFs

Sample	Aniline (g)	W (g m^{-2})	D (%)	UR (%)	k (10^{-2} S m^{-1})	PANI loading (mg cm^{-2})
PANI/ZrPP/CFs	0.5	80.37	23.88	42.11	0.40	1.55
PANI/CFs	0.5	67.92	11.65	19.26	0.00	0.71
PANI/ZrPP/CFs	1	93.13	43.55	76.80	11.53	2.83
PANI/CFs	1	75.86	24.70	40.85	0.82	1.50

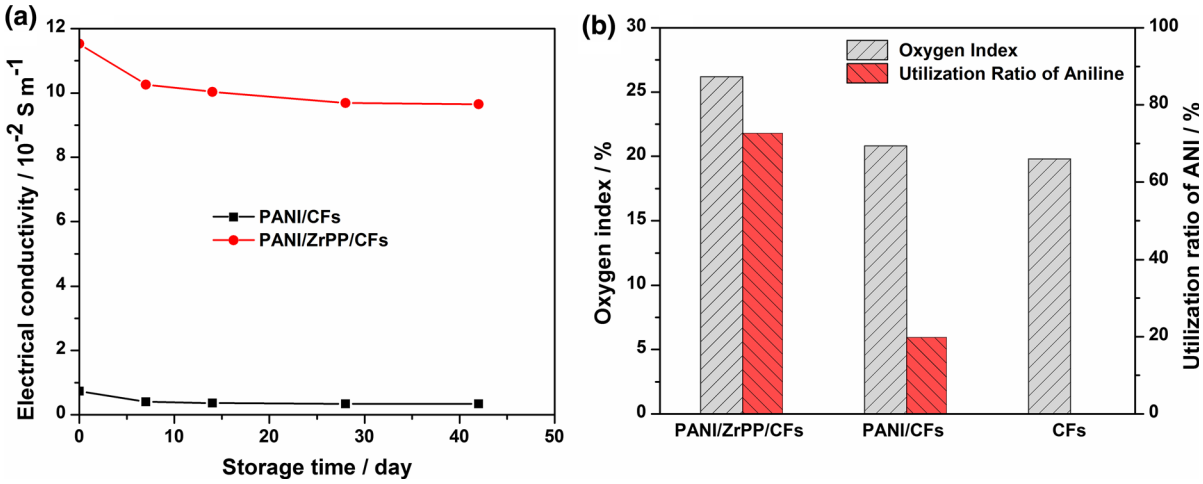

Fig. 5 Changes of electrical conductivity of paper samples made from PANI/ZrPP/CFs and PANI/CFs with storage time (**a**), Oxygen index and aniline utilization ratio of PANI/ZrPP/CFs, PANI/CFs and CFs (**b**)

addition, it may also attribute to the protection of ZrPP on CFs. The fire and heat transfer rate could be reduced by the ZrPP layer covered on the CFs surface.

Electrochemical analysis of composites

Figure 6a shows the CV curves of PANI/ZrPP/CFs electrode in a three-electrode system with the potential window ranging from − 0.1 to 0.9 V at scan rates of 0.01, 0.02, 0.05 and 0.1 V s^{-1}, respectively. PANI/ZrPP/CFs paper electrode was directly connected with the working electrode, and current collector was not used. It can be seen that there was no obvious redox peaks in the CV curves at high scan rates. This is mainly due to the polarization effect of electrode at high scan rates which may lead to the drift of redox peaks. Two pairs of redox peaks in the CV curves were exhibited by the electrode at low scan rates. It implies the reversible charge–discharge behavior and pseudo-capacitance characteristics of deposited PANI. Figure 6b shows the CV curves of the PANI/CFs and PANI/ZrPP/CFs paper electrodes at a scan rates of 0.01 V s^{-1} with the potential window ranging from − 0.1 to 0.9 V. Nearly rectangular shapes with large enclosed area were observed and there were obvious redox peaks for the electrodes, indicating that the electrodes were charged and discharged at a pseudo-constant rate over the whole CV process. The PANI/ZrPP/CFs paper electrode had a higher enclosed area than the PANI/CFs paper electrode in the CV curves. In general, the enclosed area of the CV curve is proportional to the specific capacitance of the electrode material. The increase in the specific capacitance of PANI/ZrPP/CFs paper electrode may relate to the morphology of the PANI particles. In the case of cellulose fibers modified with ZrPP, PANI particles decreased in size and uniformly covered the surface of ZrPP/CFs substrate. Such morphology can increase the contact area of the electroactive material and the electrolyte, accelerate the migration rate of the ions, and increase the specific capacitance. Figure 6c depicts GCD curves of PANI/ZrPP/CFs paper electrode at the indicated current densities. The nonlinear curves of PANI/ZrPP/CFs electrode further demonstrated the pseudo-capacitance behavior, matching well with the cyclic voltammetry curves. Symmetric charge–discharge curves exhibited at each current density showing the outstanding reversibility of redox reaction in the electrode. There was an absence of a voltage drop at the onset of the discharge curves, particularly for the scan rates more than 5 mA cm^{-2} which may be caused by the internal resistance of the paper electrode.

To compare the electrochemical performances of PANI/ZrPP/CFs and PANI/CFs paper electrodes, the GCD curves at a constant current density of 1 mA cm^{-2} are depicted in Fig. 6d. The performance of PANI/ZrPP/CFs electrode was superior to that of PANI/CFs electrode. The specific capacitances of PANI/ZrPP/CFs and PANI/CFs paper electrodes were calculated from the discharge curves based on the total mass of the active material, and the results are shown

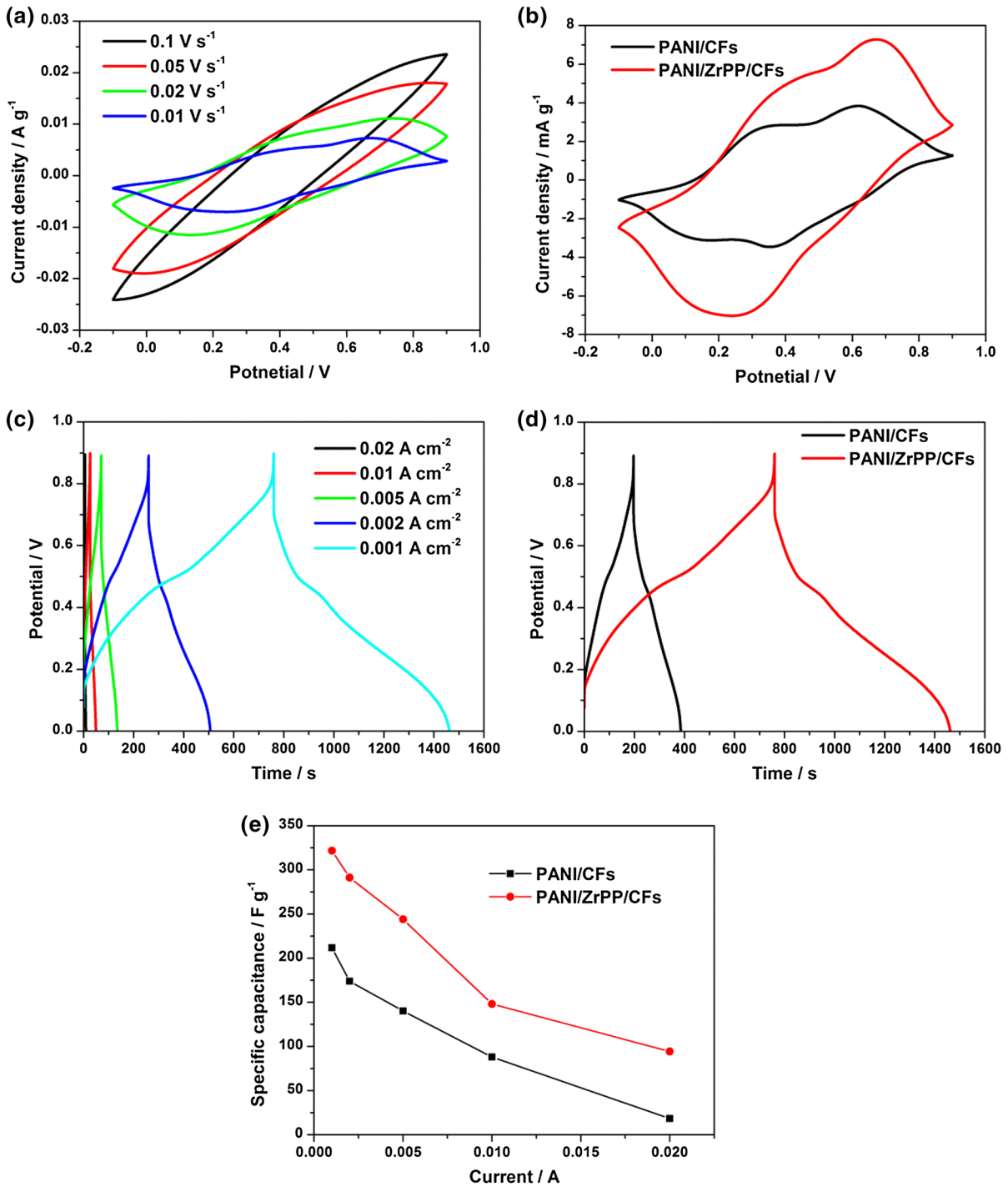

Fig. 6 Cyclic voltammograms of the PANI/ZrPP/CFs electrode at different scan rates (**a**), Cyclic voltammograms of PANI/ZrPP/CFs and PANI/CFs electrodes at a scan rate of 0.01 V s^{-1} (**b**), Galvanostatic charge–discharge profiles of the PANI/ZrPP/CFs electrode at different current densities (**c**), Galvanostatic charge–discharge profiles of PANI/ZrPP/CFs and PANI/CFs electrodes at a current density of 1 mA cm^{-2} (**d**), Specific capacitances of PANI/ZrPP/CFs and PANI/CFs electrodes at different current densities (**e**)

in Fig. 6e. The C_m values decreased with the increase of current density, and the C_m values of PANI/ZrPP/CFs electrode are higher than those of PANI/CFs electrode at each current density, which could be attributed to the modification of CFs with ZrPP. The PANI/ZrPP/CFs electrode exhibited a maximum specific capacitance of 321 F g^{-1} at 1 mA cm^{-2} and retained about 75% when the current density increased to 5 mA cm^{-2}, which is almost two times higher than that of PANI/CFs electrode. However, the C_m showed no advantage at the higher current densities and needed to be improved for practical applications. Even so, because of the low cost and facile preparation, it shows promising application in flexible energy storage devices.

The electrochemical impedance spectroscopies (EIS) of PANI/ZrPP/CFs and PANI/CFs are shown in Fig. S2a. The charge transfer resistance, which also named intrinsic ohmic resistances, are 4.09 and 6.38 Ω for PANI/ZrPP/CFs and PANI/CFs, respectively, demonstrating that PANI/ZrPP/CFs has the better conductivity and smaller charge transfer resistance at the composite electrode/electrolyte interface. Furthermore, compared with PANI/CFs, PANI/ZrPP/CFs exhibits more ideal capacitance behavior in the low frequency with a steeper line. Fig. S2b shows the cycling stability of PANI/ZrPP/CFs from GCD test at 0.005 A cm^{-2}. The C_m retention is about 78.42% after 2000 cycles, suggesting a good cycling stability.

Conclusions

Flexible PANI/ZrPP/CFs composite paper had been successfully prepared in this work. CFs were used as flexible binding substrates for ZrPP and as templates for in situ polymerization of 3D networked PANI. ZrPP was uniformly attached to the surface of CFs and enhanced the binding efficiency of aniline monomer to CFs by providing π–π interactions. The conductive PANI/ZrPP/CFs composite showed stable conductivity and outstanding flame retardancy. The electrochemical measurements proved that the incorporation of ZrPP in the paper electrode could considerably improve the capacitance. The PANI/ZrPP/CFs electrode has a specific capacitance as high as 321 F g^{-1} at 1 mA cm^{-2}. As a result, this novel composite paper may be useful for the development of energy storage and various flexible electronics and spurred an intense drive to related fields.

Acknowledgments The authors gratefully acknowledge the National Natural Science Foundation of China (Grant No. 31770620) for financial support to this work.

References

Adhikari A, Claesson P, Pan J, Leygraf C, Dédinaité A, Blomberg E (2008) Electrochemical behavior and anticorrosion properties of modified polyaniline dispersed in polyvinylacetate coating on carbon steel. Electrochim Acta 53:4239–4247. https://doi.org/10.1016/j.electacta.2007.12.069

Avelar Dutra FV, Pires BC, Nascimento TA, Mano V, Borges KB (2017) Polyaniline-deposited cellulose fiber composite prepared via in situ polymerization: enhancing adsorption properties for removal of meloxicam from aqueous media. RSC Adv 7:12639–12649. https://doi.org/10.1039/c6ra27019k

Bajgar V, Penhaker M, Martinkova L, Pavlovic A, Bober P, Trchova M, Stejskal J (2016) Cotton fabric coated with conducting polymers and its application in monitoring of carnivorous plant response. Sensors 16:498. https://doi.org/10.3390/s16040498

Berendjchi A, Khajavi R, Yousefi AA, Yazdanshenas ME (2016) Surface characteristics of coated polyester fabric with reduced graphene oxide and polypyrrole. Appl Surf Sci 367:36–42. https://doi.org/10.1016/j.apsusc.2016.01.152

Bober P, Stejskal J, Šeděnková I, Trchová M, Martinková L, Marek J (2015) The deposition of globular polypyrrole and polypyrrole nanotubes on cotton textile. Appl Surf Sci 356:737–741. https://doi.org/10.1016/j.apsusc.2015.08.105

Borgo CA, Gushikem Y (2002) Zirconium phosphate dispersed on a cellulose fiber surface: preparation, characterization, and selective adsorption of Li^+, Na^+, and K^+ from aqueous solution. J Colloid Interface Sci 246:343–347. https://doi.org/10.1006/jcis.2001.8045

de Souza Junior FG, Carlos Pinto J, Alves Garcia F, de Oliveira GE, Bruno Tavares MI, da Silva AM, Daher Pereira E (2014) Modification of coconut fibers with polyaniline for manufacture of pressure-sensitive devices. Polym Eng Sci 54:2887–2895. https://doi.org/10.1002/pen.23845

Gautam V, Singh KP, Yadav VL (2018) Preparation and characterization of green-nano-composite material based on polyaniline, multiwalled carbon nano tubes and carboxymethyl cellulose: for electrochemical sensor applications. Carbohydr Polym 189:218–228. https://doi.org/10.1016/j.carbpol.2018.02.029

Ge D, Yang L, Fan L, Zhang C, Xiao X, Gogotsi Y, Yang S (2015) Foldable supercapacitors from triple networks of macroporous cellulose fibers, single-walled carbon nanotubes and polyaniline nanoribbons. Nano Energy 11:568–578. https://doi.org/10.1016/j.nanoen.2014.11.023

Goto H (2010) Electrically conducting paper from a polyaniline/pulp composite and paper folding art work for a 3D object. Text Res J 81:122–127. https://doi.org/10.1177/0040517510377827

Hinterstoisser B, Åkerholm M, Salmén L (2003) Load distribution in native cellulose. Biomacromol 4:1232–1237. https://doi.org/10.1021/bm030017k

Hu W, Chen S, Yang Z, Liu L, Wang H (2011) Flexible electrically conductive nanocomposite membrane based on bacterial cellulose and polyaniline. J Phys Chem B 115:8453–8457. https://doi.org/10.1021/jp204422v

Hu X-S, Shen Y, Lu L-S, Xu J, Zhen J-J (2017a) Enhanced electromagnetic interference shielding effectiveness of ternary PANI/CuS/RGO composites. J Mater Sci Mater Electron 28:6865–6872. https://doi.org/10.1007/s10854-017-6386-8

Hu Y, Tong X, Zhuo H, Zhong L, Peng X (2017b) Biomass-based porous N-self-doped carbon framework/polyaniline composite with outstanding supercapacitance. ACS Sustain Chem Eng 5:8663–8674. https://doi.org/10.1021/acssuschemeng.7b01380

Kelly FM, Johnston JH, Borrmann T, Richardson MJ (2007) Functionalised hybrid materials of conducting polymers with individual fibres of cellulose. Eur J Inorg Chem 2007:5571–5577. https://doi.org/10.1002/ejic.200700608

Liu C, Zhu L, Wu H, Yang Y (2011) A novel conductivity composite based on polyaniline/zirconium phenylphosphonate. J Appl Polym Sci 119:2334–2338. https://doi.org/10.1002/app.32968

Liu X, Qian X, Shen J, Zhou W, An X (2012) An integrated approach for Cr(VI)-detoxification with polyaniline/cellulose fiber composite prepared using hydrogen peroxide as oxidant. Bioresour Technol 124:516–519. https://doi.org/10.1016/j.biortech.2012.09.002

Liu X, Zhou W, Qian X, Shen J, An X (2013) Polyaniline/cellulose fiber composite prepared using persulfate as oxidant for Cr(VI)-detoxification. Carbohydr Polym 92:659–661. https://doi.org/10.1016/j.carbpol.2012.09.083

Liu M, He S, Fan W, Miao Y-E, Liu T (2014) Filter paper-derived carbon fiber/polyaniline composite paper for high energy storage applications. Compos Sci Technol 101:152–158. https://doi.org/10.1016/j.compscitech.2014.07.008

Liu Q, Jing S, Wang S, Zhuo H, Zhong L, Peng X, Sun R (2016) Flexible nanocomposites with ultrahigh specific areal capacitance and tunable properties based on a cellulose derived nanofiber-carbon sheet framework coated with polyaniline. J Mater Chem A 4:13352–13362. https://doi.org/10.1039/C6TA05131F

Liu Q, Chen Z, Jing S, Zhuo H, Hu Y, Liu J, Zhong L, Peng X, Liu C (2018) A foldable composite electrode with excellent electrochemical performance using microfibrillated cellulose fibers as a framework. J Mater Chem A 6:20338–20346. https://doi.org/10.1039/C8TA06635C

Luo H et al (2018) Constructing 3D bacterial cellulose/graphene/polyaniline nanocomposites by novel layer-by-layer in situ culture toward mechanically robust and highly flexible freestanding electrodes for supercapacitors. Chem Eng J 334:1148–1158. https://doi.org/10.1016/j.cej.2017.11.065

MacDiarmid AG, Chiang JC, Richter AF, Somasiri NLD, Epstein AJ (1987) Polyaniline: synthesis and characterization of the emeraldine oxidation state by elemental analysis. In: Alcácer L (ed) Conducting polymers. Springer, Dordrecht. https://doi.org/10.1007/978-94-009-3907-3_9

Mao H, Wu X, Qian X, An X (2013) Conductivity and flame retardancy of polyaniline-deposited functional cellulosic paper doped with organic sulfonic acids. Cellulose 21:697–704. https://doi.org/10.1007/s10570-013-0122-1

Mao H, Liu X, Qian X, An X (2015) Preparation and dedoping-resistant effect of self-doped polyaniline/cellulose fibers (SPANI/CF) hybrid. Cellulose 22:2641–2650. https://doi.org/10.1007/s10570-015-0689-9

Mao H, Dong Y, Qian X, An X (2017) Enhancement of bonding strength of polypyrrole/cellulose fiber (PPy/CF) hybrid through lignosulfonate doping. Cellulose 24:2255–2263. https://doi.org/10.1007/s10570-017-1242-9

Maráková N et al (2017) Antimicrobial activity and cytotoxicity of cotton fabric coated with conducting polymers, polyaniline or polypyrrole, and with deposited silver nanoparticles. Appl Surf Sci 396:169–176. https://doi.org/10.1016/j.apsusc.2016.11.024

Mo Z, Zhao Z, Chen H, Niu G, Shi H (2009) Heterogeneous preparation of cellulose–polyaniline conductive composites with cellulose activated by acids and its electrical properties. Carbohydr Polym 75:660–664. https://doi.org/10.1016/j.carbpol.2008.09.010

Moon RJ, Martini A, Nairn J, Simonsen J, Youngblood J (2011) Cellulose nanomaterials review: structure, properties and nanocomposites. Chem Soc Rev 40:3941–3994. https://doi.org/10.1039/C0CS00108B

Negi YS, Adhyapak PV (2002) Development in polyaniline conducting polymers. J Macromol Sci Polym Rev 42:35–53. https://doi.org/10.1081/mc-120003094

Oksman K et al (2016) Review of the recent developments in cellulose nanocomposite processing. Compos A 83:2–18. https://doi.org/10.1016/j.compositesa.2015.10.041

Park M, Lee D, Shin S, Kim HJ, Hyun J (2016) Flexible conductive nanocellulose combined with silicon nanoparticles and polyaniline. Carbohydr Polym 140:43–50. https://doi.org/10.1016/j.carbpol.2015.12.046

Sharifi H, Zabihzadeh SM, Ghorbani M (2018) The application of response surface methodology on the synthesis of conductive polyaniline/cellulosic fiber nanocomposites. Carbohydr Polym 194:384–394. https://doi.org/10.1016/j.carbpol.2018.04.083

Shen X, Tang Y, Zhou D, Zhang J, Guo D, Friederichs G (2016) Improving the electroconductivity and mechanical properties of cellulosic paper with multi-walled carbon nanotube/polyaniline nanocomposites. J Bioresour Bioprod 1:48–54

Stein EW, Clearfield A, Subramanian MA (1996) Conductivity of group IV metal sulfophosphonates and a new class of interstratified metal amine-sulfophosphonates. Solid State Ion 83:113–124. https://doi.org/10.1016/0167-2738(95)00215-4

Stejskal J, Trchová M, Sapurina I (2005) Flame-retardant effect of polyaniline coating deposited on cellulose fibers. J Appl Polym Sci 98:2347–2354. https://doi.org/10.1002/app.22144

Tang X, Tian M, Qu L, Zhu S, Guo X, Han G, Sun K (2015) Water-repellent flexible fabric strain sensor based on polyaniline/titanium dioxide-coated knit polyester fabric. Iran Polym J 24:697–704. https://doi.org/10.1007/s13726-015-0361-0

Tissera ND, Wijesena RN, Perera JR, de Silva KMN, Amaratunge GAJ (2015) Hydrophobic cotton textile surfaces using an amphiphilic graphene oxide (GO) coating. Appl Surf Sci 324:455–463. https://doi.org/10.1016/j.apsusc.2014.10.148

Tissera ND, Wijesena RN, Rathnayake S, de Silva RM, de Silva KMN (2018) Heterogeneous in situ polymerization of polyaniline (PANI) nanofibers on cotton textiles: improved electrical conductivity, electrical switching, and tuning properties. Carbohydr Polym 186:35–44. https://doi.org/10.1016/j.carbpol.2018.01.027

Trindade IG, Martins F, Baptista P (2015) High electrical conductance poly(3,4-ethylenedioxythiophene) coatings on textile for electrocardiogram monitoring. Synth Met 210:179–185. https://doi.org/10.1016/j.synthmet.2015.09.024

Wijesena RN, Tissera ND, Perera R, Nalin de Silva KM, Amaratunga GAJ (2015) Slightly carbomethylated cotton supported TiO2 nanoparticles as self-cleaning fabrics. J Mol Catal A Chem 398:107–114. https://doi.org/10.1016/j.molcata.2014.11.012

Wu X, Qian X, An X (2013) Flame retardancy of polyaniline-deposited paper composites prepared via in situ polymerization. Carbohydr Polym 92:435–440. https://doi.org/10.1016/j.carbpol.2012.09.032

Youssef AM, El-Samahy MA, Abdel Rehim MH (2012) Preparation of conductive paper composites based on natural cellulosic fibers for packaging applications. Carbohydr Polym 89:1027–1032. https://doi.org/10.1016/j.carbpol.2012.03.044

Zhang F, Vill V, Heck J (2004) Cellulose-based polymers with long-chain pendant ferrocene derivatives as organometallic chromophores. Organometallics 23:3853–3864. https://doi.org/10.1021/om0343216